

## Polyoxometallates as Models for Oxide Catalysts

### Part II. Theoretical Semi-empirical Approach to the Influence of the Inner and Outer Mo Coordination Spheres on the Electronic Levels of Polyoxomolybdates

DANIEL MASURE,\* PATRICK CHAQUIN,\*<sup>1</sup> CATHERINE LOUIS,† MICHEL CHE,†  
AND MICHEL FOURNIER‡

\*Laboratoire de Chimie Organique Théorique (URA 506, CNRS), †Laboratoire de Réactivité de Surface et Structure (URA 1106, CNRS), and ‡Laboratoire de Physicochimie Inorganique (URA 419, CNRS), Université Pierre et Marie Curie, 4 place Jussieu, 75252 Paris Cedex 05, France

Received November 28, 1988; revised March 15, 1989

In complement to Part I, theoretical MO calculations (EHMO level) show that the main factor which influences the electronic energy levels of polyoxomolybdates is not always the local Mo symmetry (tetrahedral or octahedral). The effect of protonation and/or grafting on a surface oxide is weak but slightly larger for tetrahedral than for octahedral species and could lead to wrong attributions. The condensation of several sites in polyoxomolybdates has a greater effect since it involves a MO delocalization over the whole compound, and therefore a loss of the individuality of each octahedral or tetrahedral unit. It leads to a decrease in the HOMO-LUMO gap yielding to an absorption red shift. The effect of distortion of local symmetry by bond elongation tends to decrease the HOMO-LUMO gap in an isolated species. In a condensed system, this distortion lowers the Mo-Mo interactions and moderates the red shift due to the effect of condensation. This latter effect, however, remains predominant. © 1989 Academic Press, Inc.

#### INTRODUCTION

In the preceding paper (Part I, Ref. (1)), we examined UV-visible criteria of the assignment of the inner sphere symmetry (i.e., tetrahedral vs octahedral environment of the metal) in polyoxomolybdate compounds, on the basis of experimental results. Let us recall that the absorption wavelength is often regarded as a characteristic of the molybdenum symmetry, and is smaller for tetrahedral sites than for octahedral sites (1). It was shown in Part I that other parameters such as the aggregation of several unit cells (condensation degree) have an influence on the absorption band position and therefore that the spectroscopic criterion must be used very cautiously:

—in contrast to earlier belief, the influence of the local symmetry is negligible

compared to the farther environment of the center, particularly for large polyoxomolybdates;

—a bathochromic effect (red shift) and a broadening of the lowest energy transition band of the ligand-metal charge transfer is associated with an increasing condensation degree or with a polarizing effect of the counter cation. In the case of supported Mo catalysts, the same band broadening and red shift are expected when the Mo dispersion decreases.

Using the molecular orbital theory, we wish now to rationalize the influence on electronic energy levels of (i) the nature of the local (tetrahedral or octahedral) Mo symmetry (ii) the bond lengths and eventual protonation or grafting,<sup>2</sup> and (iii) the degree and type of condensation of several unit cells.

<sup>2</sup> For supported catalysts, chemical interaction between, for example, molybdenum oxide and an inert oxide support (such as silica, alumina, etc.).

<sup>1</sup> To whom correspondence should be addressed.

Very few theoretical studies are available in the literature about polyoxomolybdates and related compounds. A semiempirical model was proposed by Ziolkowski (2) for the determination of the active site in oxide-type catalysts, whereas the oxidation of methanol by  $\text{MoO}_3$  was investigated by Allison and Goddard (3) using a GVB method. In the same area, an approach of the olefin adsorption on  $\text{MoO}_3$  by an extended Hückel molecular orbital (EHMO)-type method was presented by Silvestre (4). A semiempirical study of some polyanions was published by Moffat (5). The bridging (Mo-X-Mo) unit in polyoxomolybdenum systems and its possible dissymmetry were extensively studied by Hoffmann *et al.* (6).

Recently, several Keggin structures ( $\text{XMo}_{12}\text{O}_{40}$ ) have been studied using model potential  $X\alpha$  methods to elucidate their reduction process and their catalytic properties (16).

Owing to the great size of the systems studied (up to  $\text{Mo}_8\text{O}_{26}^{2-}$ ), we could use only semiempirical methods of calculation which are known not to afford reliable transition energy values. However, the numerical results reported here can be regarded as indicative of the main qualitative trends that will be discussed in terms of MO perturbation and of their relative magnitude. As a landmark, at 4 eV (about 300 nm), a 0.1-eV shift corresponds to 8 nm.

The EHMO calculations were achieved using the ICON program (7). The following parameters for Mo and O atoms were used:

	Mo			O	
	5s	5p	4d	2s	2p
Coulombic (eV)	-8.77	-5.6	-11.06	-32.3	-14.8
Exponent 1	1.96	1.9	4.54	2.275	2.275
2			1.90		
Coefficient 1	1	1	0.5899	1	1
2			0.5899		

#### ORBITAL DIAGRAM OF TETRAHEDRAL AND OCTAHEDRAL UNIT CELL

The classical orbital diagram for tetrahedral  $\text{MoO}_4^{2-}$  (8) is drawn in Fig. 1a. It arises from the interaction of the 4d AOs of mo-

lybdenum and the 12 2p AOs of oxygen. The d AOs are split into two groups; the first ( $e$ ) through a destabilizing  $\pi$ -type overlap with the ligand orbital of proper symmetry, and the second destabilized to a greater extent by  $\sigma$ -type overlaps. Concerning the ligand MOs, we note that the highest one occupied (HOMO) is of  $t_1$  symmetry and is purely nonbonding as it cannot mix with any metal orbital. The second occupied MO ( $t_2$ ) set is not purely nonbonding, but the coefficients of the metal AOs are rather small (less than 0.02). The experimental UV spectrum of  $\text{Na}_2\text{MoO}_4 \cdot \text{H}_2\text{O}$  in solid state (in which  $\text{MoO}_4$  tetrahedra may be considered as isolated one from another) exhibits two absorption bands at 225 and 260 nm (9a). These bands are attributed respectively to the two ligand-metal charge transfer transitions  $t_1 \rightarrow e$  and  $t_2 \rightarrow e$  (9b). We will thus refer in the following discussion to the HOMO-LUMO gap as an index for the lowest absorption energy of the various species.

For octahedral  $\text{MoO}_6^{6-}$ , the  $t_{2g}$  ( $xy$ ,  $xz$ , and  $yz$ ) 4d AOs undergo  $\pi$ -type interactions with ligands (Fig. 1b) and are less destabilized than the  $e_g$  set. As before, the HOMO ( $t_{1g}$ ) is purely nonbonding between Mo and O, and the lower two MOs ( $t_{1u}$  and  $t_{2u}$ ) are almost nonbonding. Their relative energies, though, arise from ligand-ligand long-range second order in-phase and out-of-phase overlaps.

We will now compare the absorption wavelengths of the two single units, taking into account the differences in bond lengths: the tetrahedron  $\text{MoO}_4^{2-}$  has two  $\pi$  bonds for four bonds so the bond length should be roughly intermediate between the pure double bond (ca. 1.7 Å) and the pure single bond (ca. 1.9 to 2 Å) (10). The octahedron has only single bonds.

An increase in bond lengths lowers the  $M-L$  overlaps and hence the  $d$ -type LUMO is less destabilized, whereas the first occupied MOs are almost unaffected, due to their nonbonding character (Fig. 1). The HOMO-LUMO gap decreases for both

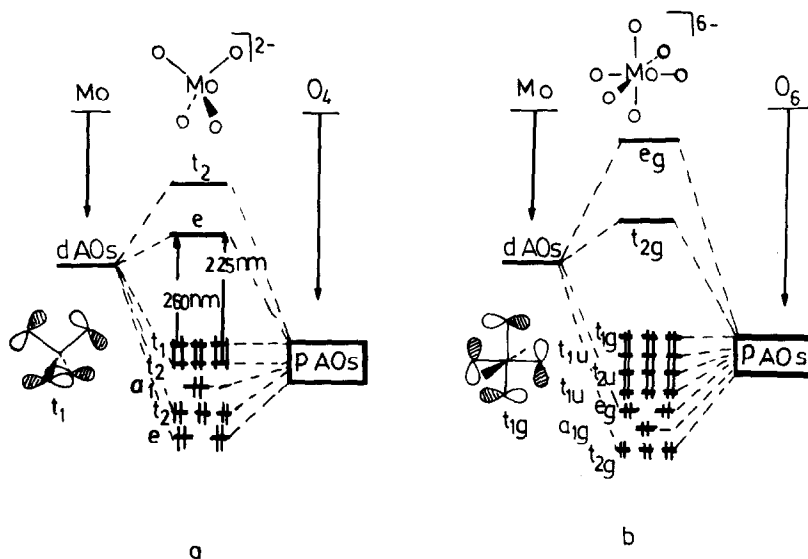


Fig. 1. Qualitative metal-ligand MO perturbation scheme of tetrahedral  $(\text{MoO}_4)^{2-}$  (a) and octahedral  $(\text{MoO}_6)^{6-}$  (b). The reported experimental absorptions are assigned according to Ref. (9a).

species as shown in Fig. 2. In addition, it can be seen that with equal bond lengths, the tetrahedral species is expected to absorb at a longer wavelength than the octahedral species. This can be easily understood if one considers that six ligands are more destabilizing than four. Taking into account the bond length differences in the two species, we see that for the reasonable values of about 1.8 Å (tetrahedron) and 1.9–2 Å (octahedron), the HOMO–LUMO gap is smaller for the octahedron than for the tetrahedron, in agreement with the experimental criterion (1).

In fact, as explained in (1), the experimental absorption energy (300–320 nm) given in the literature for octahedral species corresponds to polyoxomolybdates. Indeed, the octahedral  $\text{MoO}_6^{6-}$  unit is not known to be stable as an isolated species. Therefore, it may be asked whether the degree of condensation cannot significantly affect the absorption energy, and even become predominant over the octahedral or tetrahedral nature of the site. Moreover, other factors could be considered such as protonation, in the case of aqueous solutions of polyoxomolybdates, and grafting,

in the case of molybdenum oxide-supported catalysts. The two latter points will be examined first.

#### INFLUENCE OF PROTONATION AND GRAFTING (11)

For both octahedral and tetrahedral species, the main interaction between hydrogen and oxygen atoms arises from  $1s$ – $2p\sigma$  overlap ( $2p\sigma$  is the  $2p$  AO directed along Mo–O): the perturbation of the highest occupied  $\pi$ -type MOs is thus negligible. For

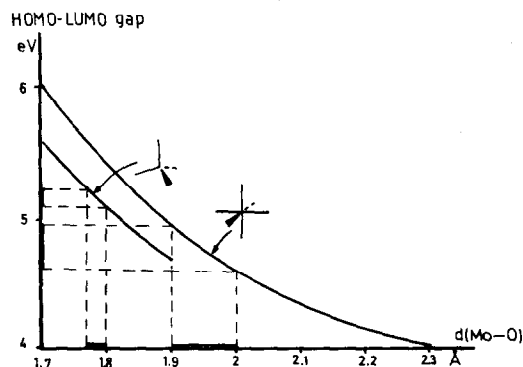


Fig. 2. Calculated HOMO–LUMO gap of octahedral and tetrahedral units as a function of bond lengths.

the same reason, the low-lying  $4d$  MOs are only slightly perturbed. We can see in Fig. 3a that, concerning the octahedral species, we observe only a weak decrease in the HOMO–LUMO gap when the number of protons increases, even though the  $O_h$  symmetry is broken. In these cases, the Mo–O bonds are always single ones and there is no significant bond length variation when bonding occurs with a hydrogen atom. On the contrary, in the  $\text{MoO}_2(\text{OH})_2$  molecule (Fig. 3b), we are now dealing with two Mo–O single bonds and two Mo=O double bonds instead of four equal “semidouble” bonds in  $\text{MoO}_4^{2-}$ . The degeneracy of the  $e$  levels is raised: one is stabilized by the increase in two bond lengths and the other is destabilized by the decrease in the other two bond lengths. Let us point out that for the monoprotonated  $\text{MoO}_4\text{H}^-$  species, the bond lengths used in the calculation result from a reasonable but somewhat arbitrary compromise, and thus the corresponding values are only indicative.

Moreover, the grafting on a support such as  $\text{SiO}_2$  is expected to produce a similar effect, as suggested by calculations performed on the model compound  $\text{MoSiO}_9\text{H}_4$  (Fig. 3b). As a matter of fact, the major effect of grafting is to replace the negative charge of an oxygen atom by a  $\sigma$  bond with a silicon atom whose electronegativity is close to that of hydrogen. So, the one-, two-, and three-proton species ( $G_1$ ,  $G_2$ , and  $G_3$ , Fig. 3) can be regarded as acceptable approximations of octahedra grafted by one, two, or three apices, respectively.

In conclusion, protonation of all sites yields a relatively weak red shift of the same order of magnitude (0.2 eV) for octahedral and tetrahedral units. Nevertheless (i) this value roughly corresponds to the HOMO–LUMO gap difference between isolated octahedron  $\text{MoO}_6^{0-}$  and tetrahedron  $\text{MoO}_4^{2-}$ ; and (ii) this shift value refers to six protons for the octahedron and only two for the tetrahedron so that the mean effect per proton is greater for the latter species. For example, both diprotonated

species  $\text{MoO}_6\text{H}_2^{4-}$  and  $\text{MoO}_4\text{H}_2$  exhibit almost the same HOMO–LUMO gap (4.87 and 4.89 eV, respectively).

#### INFLUENCE OF CONDENSATION: CHAINS OF UNIT CELLS

The results are summarized in Figs. 4–7. As we look only for qualitative trends, we have limited ourselves to a few model structures regardless of their actual existence. Chains of octahedra containing up to four units and possessing a common apex (Fig. 4) or a common edge (Fig. 5) were considered together with chains of one to four tetrahedra with a common apex (Fig. 6), and two tetrahedra with a common edge (Fig. 7, left). In addition, two structures containing both octahedra and tetrahedra (Fig. 7, right) were calculated. In all these cases, the octahedra and tetrahedra were considered as regular with standard bond lengths (1.9 Å for single bonds and 1.7 Å for double bonds). Nevertheless, the  $\text{Mo}_2\text{O}_7^{2-}$  structure with experimental bond lengths (12) was reported (see legend of Fig. 6c).

The most striking results are that (i) the energy of the HOMO is almost constant within 0.2 eV in all the models considered, and (ii) the LUMO undergoes a stabilization the magnitude of which depends on the type of chain and which increases with the degree of condensation.

The latter qualitative results can be easily explained by simple MO perturbation considerations. For example, we will examine how the relevant MOs are perturbed when two octahedra are allowed to interact through a common apex (Fig. 8). It is clear that the same reasoning would hold for tetrahedral or more condensed systems.

#### Oxygen $\pi$ -Type Nonbonding HOMO

We pointed out that (Fig. 1b) the  $(\text{MoO}_6)^{6-}$  HOMO ( $t_{1g}$ ) has a zero contribution from Mo AOs. The interaction between two units thus arises only from oxygen–oxygen long-range overlaps and is

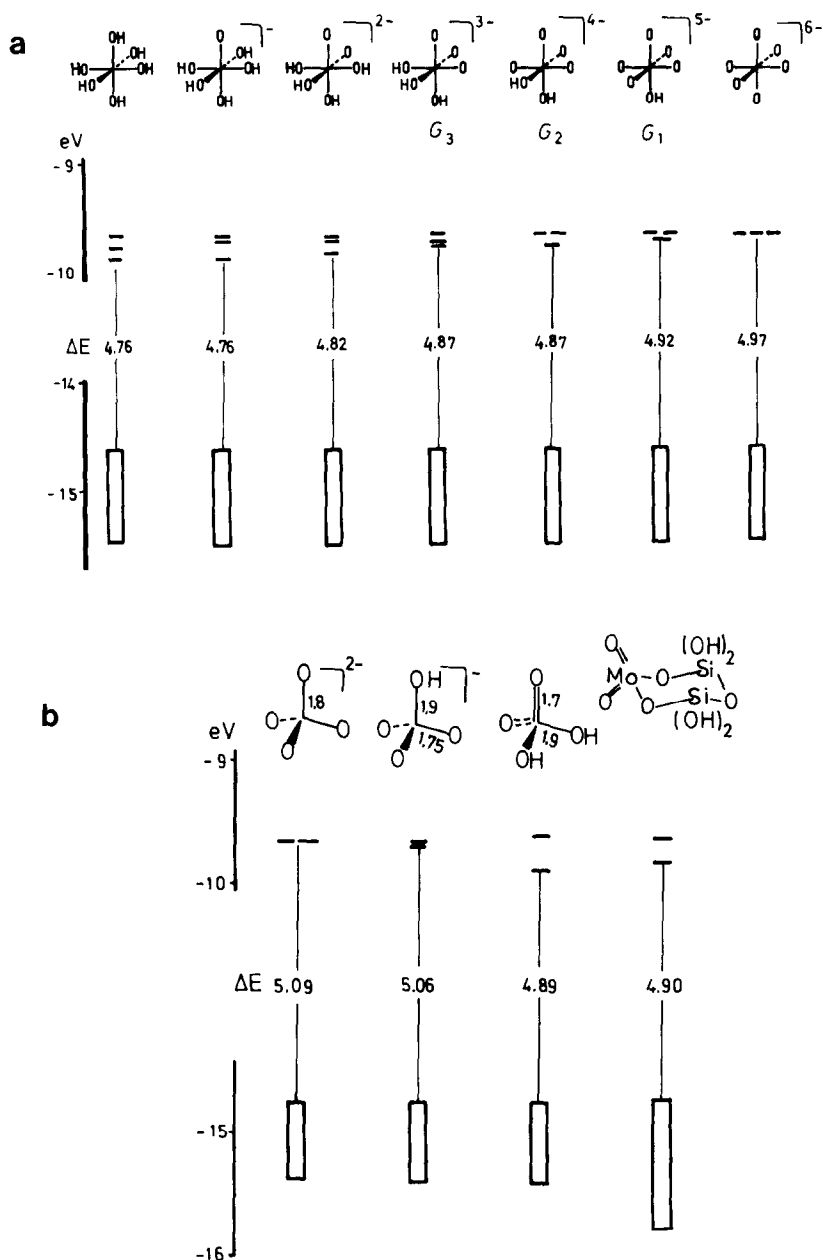


FIG. 3. Influence of protonation and grafting on ligand type (symbolized by a "box") and lowest  $d$  levels of tetrahedral (upper part) and octahedral (lower part) single units. For the latter species, the Mo-O bond lengths are taken to be equal to 1.9 Å.  $G_1$ ,  $G_2$ , and  $G_3$  represent models of the octahedron grafted by one, two, or three apices, respectively.  $\Delta E$  is the HOMO-LUMO gap.

very weak. The two in-phase and out-of-phase combinations (Fig. 8a) of  $A_{1u}$  and  $A_{2g}$  symmetry, respectively, within the  $D_{4h}$  point group, are quasi-degenerate and sepa-

rated by less than  $10^{-3}$  eV. In fact, 16 levels of various symmetries, with zero or nearly zero coefficients on the metal AOs, lie at less than 0.2 eV from the HOMO.

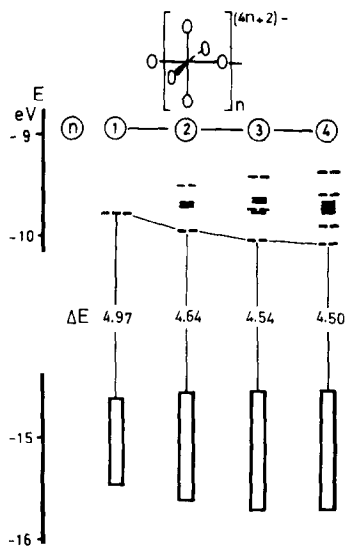


FIG. 4. Electronic levels of chains of  $n$  octahedra having a common apex ( $\text{Mo-O} = 1.9 \text{ \AA}$ ). Only the lowest  $d$  levels ( $E \leq -9 \text{ eV}$ ) are reported, and the ligand-type levels are symbolized by a "box," as in Figs. 5-7.  $\Delta E$  is the HOMO-LUMO gap.

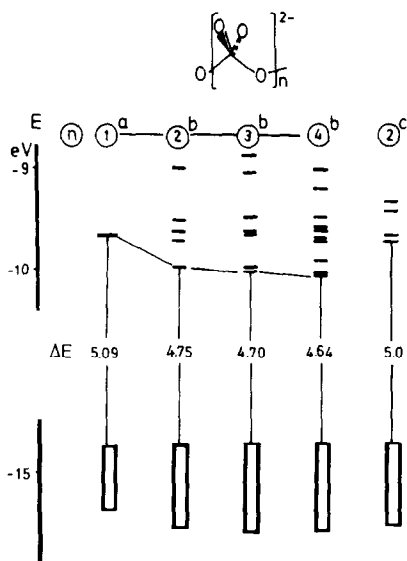


FIG. 6. Electronic levels of chains of tetrahedra with a common apex. (a) Reference unit cell ( $\text{Mo-O} = 1.8 \text{ \AA}$ ); (b)  $\text{Mo-O} = 1.9 \text{ \AA}$ ,  $\text{Mo=O} = 1.7 \text{ \AA}$ ;  $\text{Mo-O-Mo}$  and  $\text{O-Mo-O}$  angles:  $109.5^\circ$ ; (c) experimental geometry: bridging  $\text{Mo-O} = 1.876 \text{ \AA}$ , terminal  $\text{Mo-O} = 1.716 \text{ \AA}$ ,  $\text{Mo-O-Mo} = 153.6^\circ$  taken from Ref. (12).

### Molybdenum $d$ -Type LUMO

On the contrary, if we examine the lowest  $d$  level, as the coefficient of oxygen is nonzero in the  $t_{2g}$  MO of the unit cell (Fig.

1b), MOs of this type can interact through the bridging oxygen. We can discuss this interaction by considering the simplified

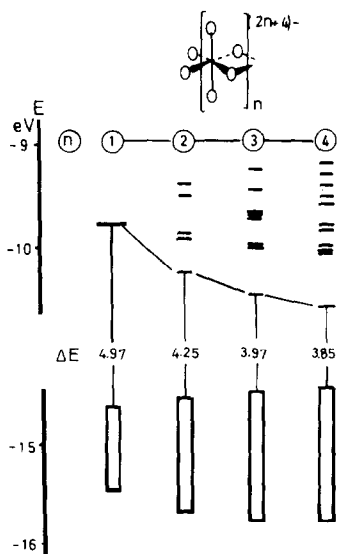


FIG. 5. Electronic levels of chains of  $n$  octahedra with a common edge. See also legend of Fig. 4.

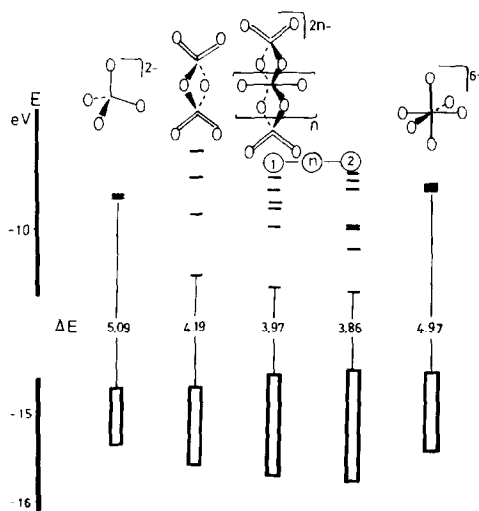


FIG. 7. Electronic levels of various species containing tetrahedra and/or octahedra. See text and caption of Fig. 4 for more details.

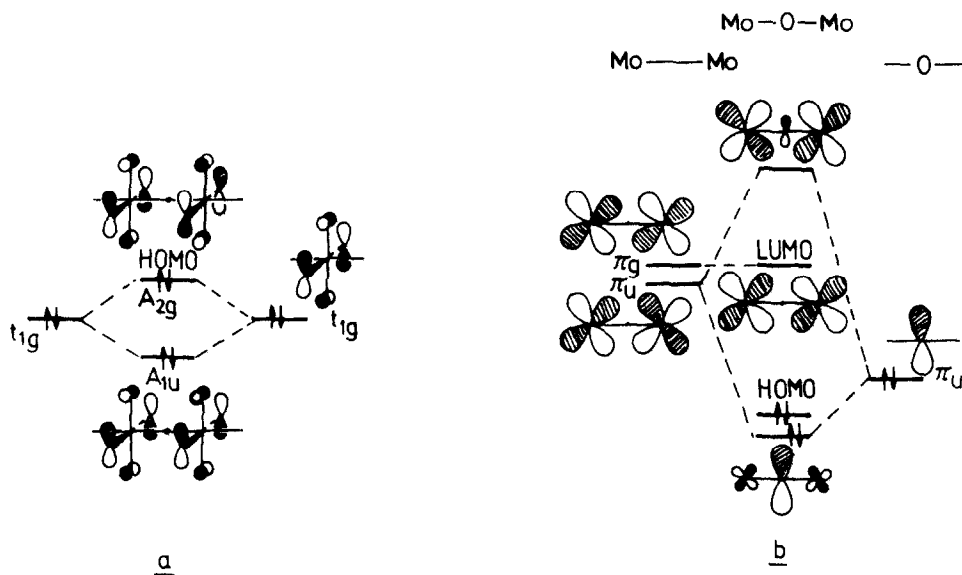


FIG. 8. Qualitative building of the relevant MOs arising from the interaction between octahedral moieties. See text for more details.

Mo-O-Mo system of the two connected octahedra (Fig. 8b). We must take into account the two  $d + d$  in-phase and out-of-phase combinations, which have nearly the same energy due to the weak  $d-d$  overlap. The MOs of the triatomic system are built by interaction of these combinations with the  $2p$  AO of oxygen. For symmetry reasons, only the  $d-d \pi_u$  combination has a nonzero overlap with oxygen, yielding a metal-type MO,  $\pi_u^*$ , antibonding between Mo and O, and a bonding ligand-type MO,  $\pi_u$ , bonding between Mo and O. Note that the latter lies below the HOMO analyzed above, due to its Mo-O bonding character. The other  $d-d \pi_g$  combination is unperturbed, and is nonbonding between the Mo atoms and the oxygen. Of course, in the full system ( $\text{Mo}_2\text{O}_{11}^{10-}$ ), antibonding contributions remain from the other 10 ligands, but one antibonding contribution (arising from the bridging oxygen) disappears in the interaction. This  $d$  level is thus stabilized in the dimer with respect to the lowest  $d$  level of the monomer.

In general terms, the condensation of an additional unit involves an extra splitting of the  $d$  levels, with lowering of the LUMO.

Since the HOMO is almost constant, the corresponding energy transition decreases when  $n$  increases, leading to a red shift in the lowest energy transition band. This is in agreement with the experimental results reported in Part I (1). This effect is asymptotically limited and we can assume from our results that this limit is reached for ca. 5 or 6 units. The effect is more pronounced when the octahedra possess a common edge because the interaction is greater. It appears from the results of Figs. 4-7 that the HOMO-LUMO gap depends more on the number of condensed unit cells than on their octahedral or tetrahedral nature. As a matter of fact, the octahedral or tetrahedral site loses its individuality when included in a large system. We will particularly note that the HOMO-LUMO gap is the same for the three octahedra edge-to-edge  $\text{O}_2(\text{MoO}_4)_3$  system (Fig. 5) as that for the system in which the terminal octahedra were replaced by two tetrahedra (Fig. 7).

#### SOME REAL ANIONS AND EFFECT OF THE DISTORTION OF THE SITES

As a guideline, and in order to emphasize the difficulties brought about by studying

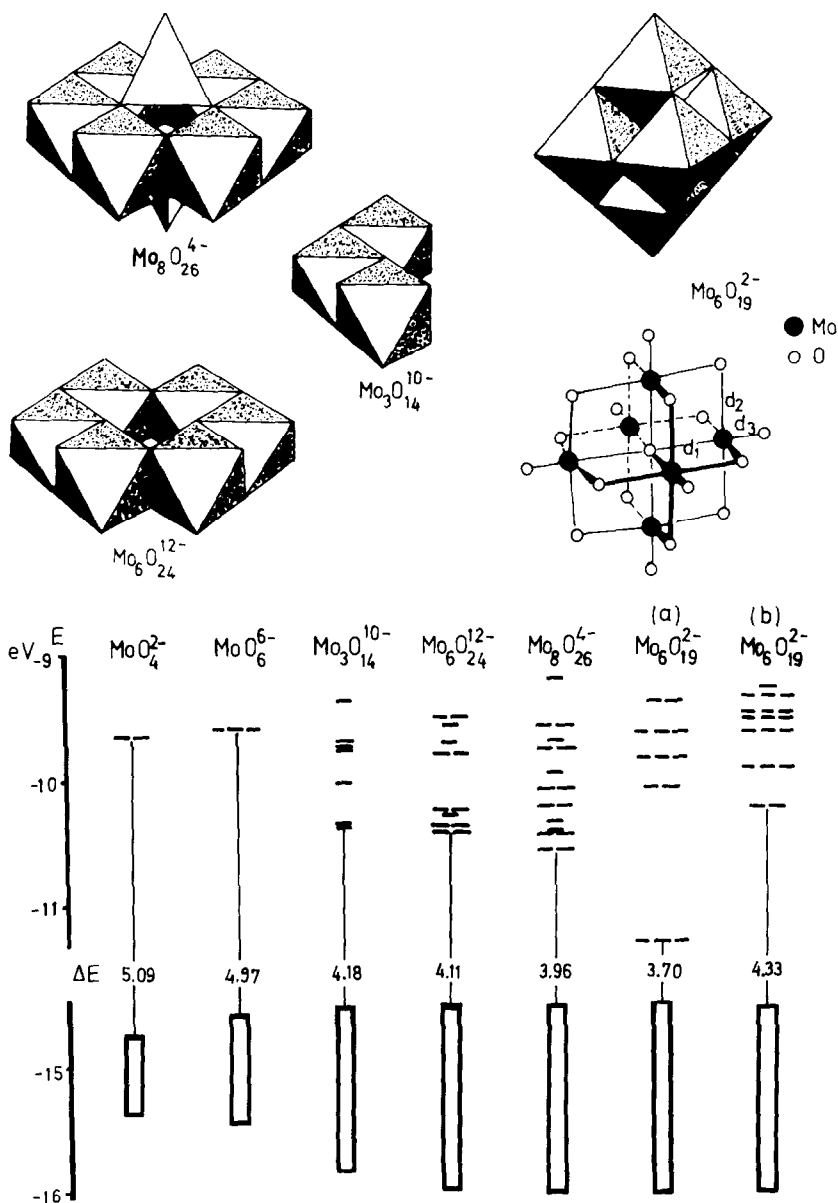


FIG. 9. Electronic levels of various polymolybdates. Except for (b), all the bond lengths have the standard values: Mo—O = 1.9 Å, Mo=O = 1.7 Å; (a) "ideal" Lindqvist structure  $d_1 = d_2 = d_3 = 1.9$  Å; (b)  $O_h$  Lindqvist structure close to experimental data  $d_1 = 2.32$  Å,  $d_2 = 1.93$  Å,  $d_3 = 1.72$  Å.

real systems, calculations for some of them are presented here. We first report (Fig. 9) model anions built from regular octahedron units ( $\text{Mo}_3\text{O}_{14}$ )<sup>10-</sup> (half-crown structure) and ( $\text{Mo}_6\text{O}_{24}$ )<sup>12-</sup> (crown). We remark that the high density of occupied and unoccupied levels allows us to expect a broadening

of the absorption bands. If two tetrahedra are added to the crown structure, yielding  $\text{Mo}_8\text{O}_{26}^{4-}$ , which actually exists, the absorption wavelength should become longer, contrary to the criterion attributing a shorter wavelength to tetrahedral isolated sites. Moreover, the LUMO coefficients



obtained from our calculations indicate that this MO is almost equally spread over the eight molybdenum atoms, so that the discrimination between octahedral and tetrahedral sites becomes meaningless. We have to specify that, in this case, the tetrahedral sites were distorted to keep Mo–O bond lengths equal to 1.9 Å. The terminal Mo=O bond length, in the tetrahedra, was taken equal to 1.7 Å.

The effects of distortion of the octahedral sites in the actual anions are exemplified in the case of the Lindqvist  $\text{Mo}_6\text{O}_{19}^{2-}$  structure (Fig. 9). The first calculation refers to an "ideal" structure formed by six regular octahedra: strong interactions between these octahedra lead to a low-energy LUMO and a small HOMO–LUMO gap. But in the actual structure (13), the central oxygen is very far from its neighboring molybdenum atoms ( $d_1 = 2.32$  Å) so that the interactions between sites become weaker, the  $d$  band tighter, and the LUMO higher.

Generally speaking, the Mo–O distance increases with increasing coordination number of the oxygen. This tends to decrease the HOMO–LUMO gap in an isolated site (Fig. 2), but it also diminishes the interaction between sites, with an opposite effect, so that the decrease of this gap by condensation is moderated. Nevertheless, the effect of condensation will always be predominant with an increase in the absorption wavelength.

#### *Other Transitions and Band Intensity*

The actual situation appears much more complex than the one we described. For example, we considered neither possible transitions other than HOMO  $\rightarrow$  LUMO nor the relative intensities of these transitions.

Indeed, the number of ligand MOs close to the HOMO increases with the degree of condensation and depends on the type of condensation. For example, 15 occupied levels lie within 0.1 eV below the HOMO for  $\text{Mo}_3\text{O}_{16}^{4-}$  (Fig. 4,  $n = 3$ ), and 10 levels

for  $\text{Mo}_6\text{O}_{24}^{12-}$  (Fig. 9). Such a situation brings up several considerations.

(i) Even if the HOMO  $\rightarrow$  LUMO transition is symmetry forbidden (i.e., of weak intensity), there is generally another allowed transition with almost the same energy.

(ii) The presence of several transitions with almost the same energy leads one to expect a broadening of the absorption bands, in agreement with experimental results (1).

(iii) The electronic transitions do not actually occur between pure electronic configurations, but between states, the description of which requires the mixing of a number of configurations. This mixing becomes more important as the electronic configurations are closer in energy.

In addition, the EHMO technique is not accurate enough for the calculation of the relative band intensities.

However, a few qualitative remarks can be drawn from our results. The presence of zero or near zero coefficients on some oxygen atoms in the LUMO indicates that the corresponding Mo–O oscillators are more directly involved in the LMCT process. As a matter of fact, the electron density previously located on these atoms is totally or almost totally transferred on molybdenum atoms when the transition occurs. In linear chains (Fig. 8), zero LUMO coefficients are found on bridging oxygens. But on other condensed systems such as Lindqvist,  $\text{Mo}_8\text{O}_{26}^{4-}$ , or  $\text{Mo}_6\text{O}_{24}^{12-}$  structures (Fig. 9) weak LUMO coefficients are found on terminal oxygens.

The latter result agrees with empirical considerations according to which the LMCT in polyoxomolybdate compounds are due to terminal Mo–O oscillators. Thus, to the first order, the intensity depends on the total number of such oscillators. This is experimentally verified on TBA salts of  $\text{Mo}_6\text{O}_{19}^{2-}$  (Fig. 9),  $\text{PMo}_{12}\text{O}_{40}^{3-}$ , and  $\text{P}_2\text{Mo}_{18}\text{O}_{62}^{6-}$ , having 6, 12, and 18 terminal Mo–O, respectively. The integrated in-

tensity (in arbitrary units) has been found equal to 1.6, 2.0, and 2.4 per terminal Mo–O, respectively, which is almost constant (14). To the second order, the observed increase in the intensity per Mo–O along this series with increasing condensation degree may be taken into account. It can be tentatively interpreted using MO considerations. If we consider a single Mo–O oscillator, the HOMO is a pure ligand  $p$  oxygen AO. The  $d$ -type metal LUMO is an antibonding mixing of  $d$  and  $p$  AOs, namely  $c_1d - c_2p$ , where  $c_1$  and  $c_2$  are positive numbers and  $c_1 > c_2$ . Thus, the corresponding transition moment can be written

$$\begin{aligned} \langle \text{HOMO} | \mathbf{r} | \text{LUMO} \rangle &= \langle p | \mathbf{r} | c_1d - c_2p \rangle \\ &= c_1 \langle p | \mathbf{r} | d \rangle - c_2 \langle p | \mathbf{r} | p \rangle. \end{aligned}$$

The transition probability, proportional to the square of the transition moment, is thus maximum when  $c_2$  vanishes. More intuitively, if the HOMO is pure ligand and the LUMO is pure metal, the HOMO  $\rightarrow$  LUMO transition corresponds to the strongest charge transfer. Our calculations show that the LUMO energy decreases with the degree of condensation by decreasing in antibonding participation of the ligands (i.e., decrease in  $c_2$ -like coefficients). We can thus expect an increase in the absorption intensity with the condensation, all other things being equal. (For example, we should compare symmetry-allowed transitions.) In any case, we have to be very cautious owing to the poor resolution of the absorption spectra (1) which do not provide a reliable set of experimental data for the study of band intensities.

#### *Relation between Electronic Absorption and Redox Properties*

Although this topic is beyond our purpose, an interesting relation can be made between the absorption wavelength and the first reduction potential of these species (15).

As the HOMO remains almost constant, the HOMO–LUMO gap reveals the ability of the metal to accept an additional elec-

tron. It can be related to the redox potential providing the latter can be determined in reversible conditions on nonsolvated systems. These requirements are fulfilled with polyanion clusters in unreduced form. The Lindqvist structure (Fig. 9)  $\text{Mo}_6\text{O}_{19}^{2-}$  has a first reduction process (vs SCE) at  $-0.55$  V,  $\text{SiMo}_{12}\text{O}_{40}^{4-}$  at  $-0.45$  V, and  $\text{P}_2\text{Mo}_{18}\text{O}_{62}^{6-}$  at  $-0.34$  V (14). The single-octahedron unit  $\text{MoO}_6^{6-}$  is unknown, but its reduction potential can be evaluated at ca.  $-2$  to  $-3$  V. These results agree with the general trends we can deduce from our calculations: first, the compounds are expected to be more reducible when the degree of condensation increases, and second, the potential asymptotically tends to a limit for a certain number of condensed units which depends on the type of condensation.

#### CONCLUSION

In Part I (1), the analysis of the UV–visible spectra of model polyoxomolybdates with well-known structures indicates that the earlier attributions of the absorption bands of supported Mo catalysts must be reconsidered.

These conclusions are confirmed in this paper on the basis of theoretical MO calculations. They show that the main factor which influences the electronic energy levels of polyoxomolybdates is not always the local Mo symmetry (tetrahedral or octahedral) when Mo centers interact. The condensation of several Mo units has a great effect on the energy levels: it involves a MO delocalization over the whole compound, and therefore a loss in individuality of each tetrahedral or octahedral unit. It leads to a decrease in the HOMO–LUMO gap, yielding to a red shift in the absorption band. A band broadening can also be expected due to the splitting of the low-lying empty  $d$  levels.

In addition, this paper has shown that:

—the effect of protonation or grafting on  $\text{SiO}_2$  is weak, but slightly larger for tetrahedral than for octahedral isolated species. It

could nevertheless be large enough to lead to a confusion in the assignment of the type of symmetry.

—the effect of distortion of local symmetry by bond elongation tends to decrease the HOMO–LUMO gap for an isolated species. In a condensed system, this distortion lowers the Mo–Mo interactions and moderates the red shift due to the effect of condensation. However, this latter effect remains predominant.

#### REFERENCES

1. Fournier, M., Louis, C., Che, M., Chaquin, P., and Masure, D., *J. Catal.* **119**, 400 (1989), and references therein.
2. Ziolkowski, J., *J. Catal.* **80**, 263 (1983); *J. Catal.* **84**, 317 (1983).
3. Allison, J. N., and Goddard, W. A., *J. Catal.* **92**, 127 (1985).
4. Silvestre, J., *J. Amer. Chem. Soc.* **109**, 594 (1987).
5. Moffat, J. B., *J. Mol. Catal.* **26**, 385 (1984).
6. Wheeler, R. A., Whangbo, M.-H., Hughbanks, T., Hoffmann, R., Burdett, J. K., and Albright, T. A., *J. Amer. Chem. Soc.* **108**, 2222 (1986).
7. Hoffmann, R., and Lipscomb, W. N., *J. Chem. Phys.* **36**, 2179 (1962); *J. Chem. Phys.* **37**, 2872 (1962); Hoffmann, R., *J. Chem. Phys.* **39**, 1397 (1963); Wolsberg, M., and Helmoltz, J., *J. Chem. Phys.* **20**, 837 (1952).
8. Ballhausen, C., and Liehr, A., Jr., *J. Mol. Spectrosc.* **2**, 342 (1958); *J. Mol. Spectrosc.* **4**, 190 (1960); Ballhausen, C., "Ligand Field Theory," p. 242. McGraw–Hill, New York, 1962.
9. (a) Ashley, J. H., and Mitchell, P. C. H., *J. Chem. Soc. A*, 2821 (1968); (b) Israeli, Y. J., *Bull. Soc. Chim. Fr.*, 2692 (1965). See also Bartecki, A., and Dembicka, D., *J. Inorg. Nucl. Chem.* **29**, 2907 (1967).
10. Fuchs, J., and Knoepfadel, I., *Z. Kristallogr.* **158**, 165 (1982).
11. For a review on quantum models of chemisorption on oxide catalysts, see Zhidomirov, G. M., and Kazansky, V. B., in "Advances in Catalysis" (D. D. Eley, H. Pines, and P. B. Weisz, Eds.), Vol. 31, p. 131. Academic Press, New York, 1982.
12. Day, V. W., Fredrich, M. F., Klemperer, W. G., and Schum, W., *J. Amer. Chem. Soc.* **99**, 6146 (1977).
13. The actual structure is slightly distorted with respect to  $O_h$  symmetry. This distortion is not significant in our purpose and mean Mo–O bond lengths were taken from: Nagano, O., and Sasaki, Y., *Acta Crystallogr. Sect. B* **35**, 2387 (1979); Alcock, R., Bissell, E. C., and Shawl, E. T., *Inorg. Chem.* **12**, 2963 (1973); Garner, D. C., Howlader, N. C., Mabbs, F. E., McPhail, A. T., Miller, R. W., and Ouan, K. D., *J. Chem. Soc. Dalton*, 1582 (1978).
14. Fournier, M., unpublished results.
15. This discussion has been suggested by a referee.
16. Teketa, H., Katsuki, S., Eguchi, K., Seiyama, T., and Yamazoe, N., *J. Phys. Chem.* **90**, 2959 (1986); Eguchi, K., Seiyama, T., Yamazoe, N., Katsuki, S., and Taketa, H., *J. Catal.* **111**, 336 (1988).